

Near-optimal protocols in complex nonequilibrium transformations

Todd R. Gingrich,^{1,2,*} Grant M. Rotskoff,^{3,†} Gavin E. Crooks,^{4,5,‡} and Phillip L. Geissler^{2,6,§}

¹*Physics of Living Systems Group, Department of Physics,
Massachusetts Institute of Technology, 400 Technology Square, Cambridge, MA 02139*

²*Department of Chemistry, University of California, Berkeley, CA 94720, USA*

³*Biophysics Graduate Group, University of California, Berkeley, CA 94720, USA*

⁴*Physical Biosciences Division, Lawrence Berkeley National Laboratory, Berkeley, CA 94720, USA*

⁵*Kavli Energy NanoSciences Institute at Berkeley, CA 94720, USA*

⁶*Chemical Sciences Division, Lawrence Berkeley National Laboratory, Berkeley, CA 94720, USA*

The development of sophisticated experimental tools for controlling nanoscale systems has motivated efforts to design driving protocols which minimize the energy dissipated to the environment. Computational models are a crucial ingredient in this practical challenge. We describe a general method for sampling an ensemble of finite-time, nonequilibrium protocols biased towards a low average dissipation. We show that this scheme can be carried out very efficiently in several limiting cases. As an application, we sample the ensemble of low-dissipation protocols that invert the magnetization of a 2D Ising model and explore how the diversity of the protocols varies in response to constraints on the average dissipation. In this example, we find that the set of near-optimal protocols is surprisingly large.

When a system is guided gradually from one equilibrium state to another, the amount of heat dissipated into its surroundings is insensitive to the manner of driving. In the more realistic case of an irreversible transformation in finite time, however, the dissipation can vary greatly from one driving protocol to another. These basic tenets of thermodynamics have received renewed attention in recent years due to improved capabilities for manipulating systems at small scales [1–7] and advances in the theoretical understanding of nonequilibrium fluctuations [8–10]. In particular, many studies have sought to identify which finite-time protocols transform a system with the minimum amount of dissipation [11–18]. Protocols which are optimal in this sense provide the most efficient route to measuring equilibrium free energy differences—in simulations and in experiments [19]—via the Jarzynski relation [14, 20]. Low-dissipation protocols also provide insight into the optimal design of nanoscale machines, both synthetic [4, 5] and natural [21].

In practice, it is not possible to identify the optimal protocol for complex, many-body systems driven far-from-equilibrium. Our inability to compute strictly optimal protocols motivates a pragmatic question: how large is the set of nearly optimal protocols? In this paper we develop a framework to measure that set. We introduce an entropy which indicates how many different protocols realize the same value of dissipation. For low values of dissipation, this protocol entropy quantifies how prevalent the near-optimal protocols are, highlighting when the system may be efficiently driven in many different ways. In analogy with common techniques of statistical physics, we present Monte Carlo methods to numerically compute the entropy by sampling protocols with a preference for low dissipation. The samples generated by this procedure demonstrate the distinct ways in which the system can be driven while maintaining the expect-

tation of low dissipation. Variation among the sampled protocols accentuates features that are unimportant for ensuring low dissipation; similarly, the lack of variation highlights features that are essential for this goal.

We illustrate the protocol-sampling framework with a numerical study of spin inversion of a ferromagnet, an essential process for copying information encoded in magnetic storage devices. Reduction of dissipation in this context is important because the thermodynamic costs of copying and erasing bits is projected to account for a significant fraction of future computational energy costs [22, 23]. We examine a simple microscopic model of this system, the two-dimensional Ising model (see Fig. 1). At low temperature and in the presence of an external magnetic field, magnetic domains align in the direction of the field. By adjusting the magnetic field and the temperature as functions of time, the magnetization may be rapidly inverted with a dissipation that depends on the manner in which the field and temperature are changed. Analysis of the protocol entropy in this model indicates that a surprisingly large set of non-optimal protocols can be used to control the system with a dissipation comparable to that associated with the optimal protocol.

Protocol entropy

We first consider an ensemble of protocols $\Lambda(t)$ sharing the same value ω of average dissipation. The protocol entropy $S(\omega)$ of this ensemble measures the density of protocols which have mean dissipation ω . In analogy to the standard microcanonical ensemble of statistical mechanics, we write the entropy as

$$S(\omega) = \ln \left[\Omega_0 \int \mathcal{D}\Lambda(t) \delta(\omega - \langle \omega \rangle_\Lambda) \right], \quad (1)$$

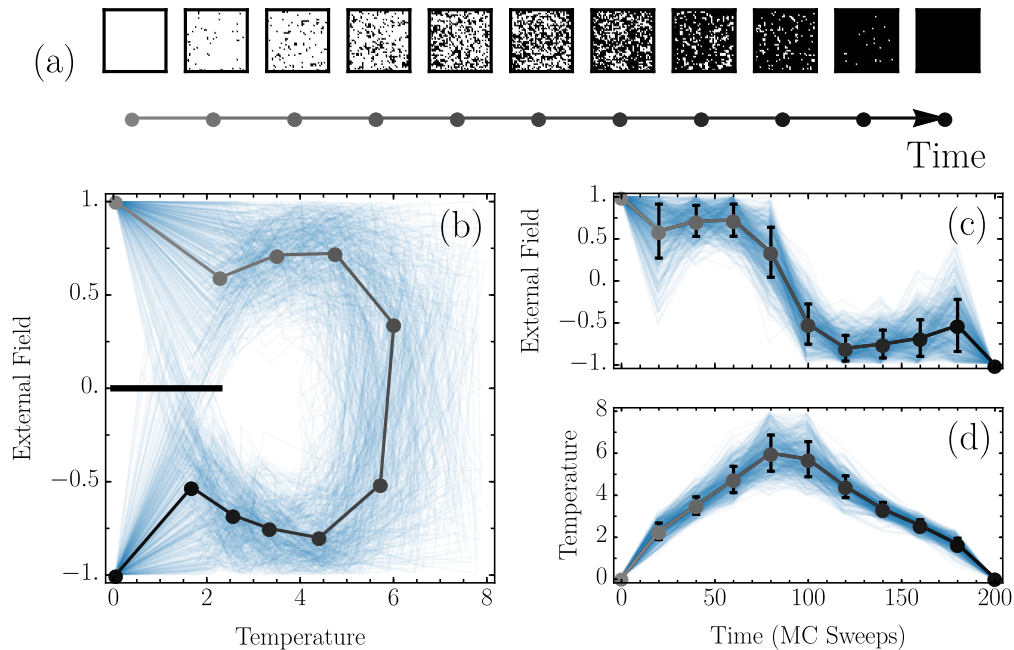


FIG. 1. *Low-dissipation protocols that invert a 2D Ising magnet in finite time.* (a) Snapshots of the 40×40 periodically replicated magnet during field inversion. (b) 450 representative samples of low-dissipation protocols (blue), collected from the $\lambda = 0.5, N = 5$ protocol ensemble, (5) Protocols are constructed from ten 20-sweep-long linear ramps in the temperature and field. (c) The external field as a function of time. (d) The temperature as a function of time. In panels (b)-(d) lines ranging from gray to black indicate averages over the 450 protocols, with shading corresponding to the times of the snapshots in (a).

where the integral runs over the space of time-dependent protocols $\Lambda(t)$ and Ω_0 is a constant which sets the arbitrary zero of entropy. The delta function is the density of protocols whose average dissipation $\langle \omega \rangle_\Lambda$ lies within an infinitesimal interval around the specified value of ω . The Λ subscript denotes an average taken over the probability distribution $P_{\text{traj}}[x(t)|\Lambda(t)]$ of stochastic trajectories evolving under the fixed protocol $\Lambda(t)$,

$$\langle \omega \rangle_\Lambda = \int \mathcal{D}x(t) P_{\text{traj}}[x(t)|\Lambda(t)] \omega[x(t), \Lambda(t)]. \quad (2)$$

For a single trajectory $x(t)$ the dissipation ω can be cast in terms of an imbalance between forward and reversed dynamics [10] with,

$$\omega[x(t), \Lambda(t)] = \ln \frac{P_{\text{traj}}[x(t)|\Lambda(t)]}{P_{\text{traj}}[\tilde{x}(t)|\tilde{\Lambda}(t)]}. \quad (3)$$

Tildes signify time-reversal, so the numerator and denominator are probabilities of forward and reverse trajectories, respectively.

Optimal protocols, which carry some minimal dissipation, represent a small fraction of the possible protocols. Consequently, the protocol entropy evaluated at this minimal dissipation is low. As the dissipation increases, the entropy increases, and the growth rate reflects how flexibly low-dissipation protocols may be constructed. In par-

ticular, rapid entropic growth near the minimum dissipation suggests that targeting an exact optimal protocol is both challenging and gratuitous. Many other protocols, in practice, will perform comparably to the optimum.

A canonical protocol ensemble

To compute the protocol entropy, it is useful to introduce a canonical protocol ensemble

$$P_{\text{canon}}[\Lambda(t)] \propto e^{-\gamma \langle \omega \rangle_\Lambda}. \quad (4)$$

In correspondence with the canonical ensemble of statistical mechanics, $\langle \omega \rangle_\Lambda$ acts as an effective energy for each protocol and γ plays the role of inverse temperature, tuning the mean dissipation (i.e., the average of ω over the distribution P_{canon}). Searching for a protocol with strictly minimum dissipation amounts to a zero “temperature” ($\gamma \rightarrow \infty$) quench while near-optimal protocols are identified by large (finite) values of γ .

We compute the protocol entropy by sampling the canonical ensemble defined by (4). We sample using several different biasing strengths γ and combine the data to calculate $S(\omega)$ over a broad range. In addition to obtaining $S(\omega)$ those protocols sampled from (4) are instructive. When using a large enough γ , the sampled pro-

ocols reveal representative low-dissipation ways to drive the nonequilibrium system.

Sampling protocols and trajectories

In principle, the ensemble defined by (4) may be directly sampled with a Monte Carlo procedure that conditionally accepts protocol changes based on the corresponding changes in $\langle\omega\rangle_\Lambda$. For complex systems, however, values of $\langle\omega\rangle_\Lambda$ are typically not known exactly. They can be estimated from the sample mean $\bar{\omega}_\Lambda = N^{-1} \sum_i \omega[x_i(t)|\Lambda(t)]$ of a collection of N trajectories drawn from $P_{\text{traj}}[x(t)|\Lambda(t)]$. But for finite N , replacing $\langle\omega\rangle_\Lambda$ by $\bar{\omega}_\Lambda$ in (4) yields a distribution of protocols which differs from $P_{\text{canon}}[\Lambda(t)]$. Strategies to correct for the finite- N bias have been formulated to enable conventional Boltzmann sampling when configurational energies cannot be calculated with certainty [24–28]. Here, we consider an analogous strategy in the context of sampling protocols.

To sample the canonical protocol distribution, we construct a Monte Carlo procedure which performs a random walk through the joint space of protocols and N independent trajectories $x_1(t), x_2(t), \dots, x_N(t)$. A trial move amounts to an attempt to make changes in both $\Lambda(t)$ and in $\{x_i(t)\}$. Operationally, this proposed change can be achieved by first perturbing the protocol with a symmetric generation probability before regenerating the trajectories using the new protocol. For simplicity, we consider the case that the trajectory generation probabilities are symmetric, as in the noise-guided shooting procedures of transition path sampling [29–31]. Accepting a trial move with the Metropolis probability $\min[1, \exp(-\lambda\Delta\bar{\omega})]$, where $\Delta\bar{\omega}$ is the difference between the sample means under the original and trial protocols, yields a stationary distribution

$$P_{\text{sampled}}[x_1(t), \dots, x_N(t), \Lambda(t)] \propto \exp\left(-\frac{\lambda}{N} \sum_{i=1}^N \omega[x_i(t)|\Lambda(t)]\right) \quad (5)$$

The resulting marginal distribution of protocols,

$$P_{\text{sampled}}[\Lambda(t)] \propto \left\langle e^{-\lambda\omega/N} \right\rangle_\Lambda^N, \quad (6)$$

is determined by the dissipation statistics of each protocol, but in a more complicated way than P_{canon} . Nevertheless, we show that the sampled protocols are drawn from a canonical protocol distribution in two special situations: the case of Gaussian dissipation distributions and the large N limit.

Cumulant expansion

The expression for the marginal distribution (6) may be recast as

$$P_{\text{sampled}}[\Lambda(t)] \propto e^{N\psi_\Lambda(-\lambda/N)}, \quad (7)$$

where $\psi_\Lambda(k) = \ln \langle e^{k\omega} \rangle_\Lambda$ is the cumulant generating function for the dissipation. A cumulant expansion,

$$\psi_\Lambda(-\lambda/N) = -\frac{\lambda \langle\omega\rangle_\Lambda}{N} + \frac{\lambda^2 \langle\delta\omega^2\rangle_\Lambda}{2N^2} - \mathcal{O}\left(\frac{\lambda^3}{N^3}\right), \quad (8)$$

relates the probability of sampled protocols to the cumulants of the dissipation distribution $P(\omega|\Lambda(t))$, where $\delta\omega = \omega - \langle\omega\rangle_\Lambda$. As N grows, the contribution from higher order cumulants will fall off so long as highly order cumulants grow in a bounded way. For sufficiently large N , the difference between sampling (4) and (5) clearly vanishes because the sample mean converges to the average dissipation.

In the special case that $P(\omega|\Lambda(t))$ is Gaussian distributed for each protocol $\Lambda(t)$, a powerful simplification arises, averting the need to work in the limit of large N . Gaussian dissipation distributions occur in many contexts—as a defining feature of linear response [32], in the limit of slow adiabatic driving [32], and when Brownian particles evolve in driven harmonic potentials [33]. In all these cases, the cumulants beyond the variance vanish, allowing us to exactly truncate (8) at second order. If we further take $\Lambda(t)$ to be symmetric under time reversal, then the fluctuation theorem provides an exact relationship between the mean and variance: $\langle\delta\omega^2\rangle_\Lambda = 2\langle\omega\rangle_\Lambda$. As a result, the biased protocol distribution can be expressed in terms of mean dissipation alone,

$$P_{\text{Gaussian}}[\Lambda(t)] \propto e^{-\lambda(1-\frac{1}{N})\langle\omega\rangle_\Lambda}. \quad (9)$$

(9) has precisely the form of the canonical protocol distribution (4), with an effective bias $\gamma = \lambda(1 - \lambda/N)$. This result offers great flexibility. An exact bias towards low average dissipation can be achieved with any N , e.g., by sampling a small number of trajectories for each proposed change in protocol. Since generating trajectories dominates the computational expense of our sampling scheme, the freedom to choose small N is very attractive.

The limitation with using small N when sampling protocols is that the achievable bias strength γ is bounded from above by $\gamma_{\text{max}} = N/4$. This constraint reflects a generic feature of the cumulant generating function $\psi_\Lambda(k)$, namely its symmetry about $k = -1/2$ [34]. $P_{\text{sample}}[\Lambda(t)]$ is correspondingly symmetric in λ about $\lambda = N/2$. Larger values of λ emphasize trajectories with negative dissipation, which are necessarily atypical of the distribution $P[x(t)|\Lambda(t)]$ according to the second law of thermodynamics. Rather than favoring protocols that yield smaller dissipation on average, sampling with

$\lambda > N/2$ generates rare trajectories which are characteristic of the reverse-time dynamics. Moreover, sampling with values of λ approaching $N/2$ requires generation of increasingly rare trajectories, complicating efficient path sampling as discussed in the Supporting Information (SI).

RESULTS

Spin inversion protocols

To illustrate the use of the low-dissipation protocol ensemble, we consider the inversion of spins in a ferromagnet. We imagine initializing a ferromagnet at low temperature, thereby ensuring alignment of the magnet into a well-defined “up” or “down” state. Within this particular physical system, we ask how to best reverse the bit. That is, how should we vary the temperature and external field as functions of time to flip the state of the magnet without excess dissipation? This problem, relevant to the design of low power magnetic hard drives, has been investigated as an optimal control problem elsewhere [35, 36]. Here we also consider the near-optimal drivings.

We model the ferromagnet as a two-dimensional Ising model with periodic boundary conditions and dynamics generated by a succession spin flips, which are conditionally accepted according to the Glauber criterion. With an external magnetic field h , the energy of a configuration is given by

$$E = h \sum_i \sigma_i - \sum_{\langle ij \rangle} \sigma_i \sigma_j, \quad (10)$$

where $\sigma_i = \pm 1$, and $\langle ij \rangle$ indicates a sum over nearest neighbor sites i and j . An attempted spin flip which alters the energy by ΔE is accepted with probability $e^{-\Delta E/T}/(1 + e^{-\Delta E/T})$, with T the dimensionless temperature of the bath. Unlike equilibrium Ising model dynamics, the temperature and magnetic field are time-dependent as prescribed by a nonequilibrium protocol $\Lambda(t) = \{T(t), h(t)\}$. In a finite amount of time t_{obs} we aim to switch from the macroscopic up state to the down state, so we consider only protocols satisfying $T(0) = T(t_{\text{obs}}) = 0.05$ and $h(0) = -h(t_{\text{obs}}) = 1$.

One consequence of the nonequilibrium driving is that the dynamics is not microscopically reversible. For ordinary Glauber dynamics, the probability of some sequence of spin flips exactly equals the probability of the time-reversed sequence of flips, but the time-dependent driving breaks this equality. By tracking the random numbers which generate each spin flip, we explicitly compute the forward and time-reversed probabilities of each trajectory, thereby computing the stochastic thermodynamic dissipation via (3). Physically, the dissipation of each microscopic step multiplied by T is the heat transferred from the thermal bath into the system.

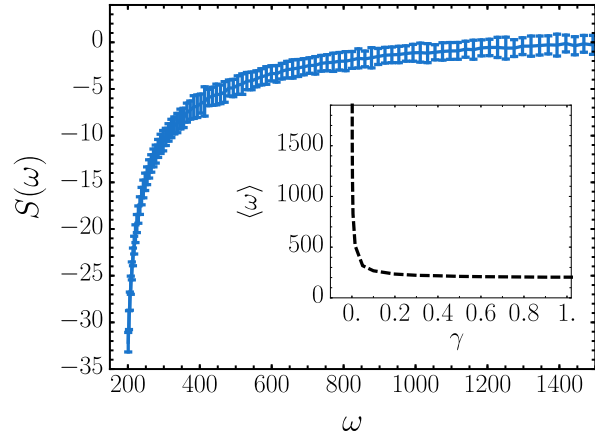


FIG. 2. Protocol entropy quantifies the diversity of protocols with average dissipation ω . By sampling the distribution (4) with $t_{\text{obs}} = 200$ MC sweeps and using various biasing strengths γ , the protocol entropy $S(\omega)$ was computed using the Multistate Bennett Acceptance Ratio (MBAR) method [37]. The slope of the protocol entropy at $\omega = \langle \omega \rangle$ gives the strength of the bias necessary to yield mean dissipation $\langle \omega \rangle$. Inset: The average dissipation for protocols as a function of the bias γ . Note that a small bias produces most of the achievable dissipation reduction.

We use Monte Carlo techniques, discussed further in the Methods section, to sample low-dissipation protocols from (5) with $\lambda = 0.5, N = 5$. Fig. 1 shows 450 representative protocols, which share the principal feature that they skirt around the Ising model critical point. Protocols that pass near the critical point are particularly dissipative [36], because critical slowing down causes the spin system to lag behind the control parameters. These protocols are thus atypical under the low dissipation bias. Roughly, the optimal strategy requires that we first heat the magnet, then invert the field, then cool the magnet, but the varied protocols in Fig. 1 demonstrate significant leeway in how these steps are carried out. Most notably, while the system is held at low temperature, the magnetic field need not be precisely tuned, as evidenced by large variations both early and late in the protocol. These field variations, insufficient to overcome spin-spin coupling, do not typically invert individual spins; they involve little work and therefore little dissipation.

Protocol Entropy

The protocol entropy, which reflects diversity of low-dissipation protocols, is shown for the spin inversion problem in Fig. 2. Near the apparent minimum dissipation, a small increase in mean dissipation is accompanied by a steep rise in $S(\omega)$, i.e., the number of protocols grows rapidly as we permit modest excess dissipation. In fact, the density of protocols increases by several orders of

magnitude for a change in dissipation that is very small relative to dissipation fluctuations for a fixed protocol. Farther from the minimal value of mean dissipation, the protocol entropy climbs much more gradually.

The slope of $S(\omega)$ reflects the strength of bias γ needed to depress the average dissipation. The inset of Fig. 2 illustrates a crossover between two regimes: small biases greatly reduce the mean dissipation but further reduction requires very large biases. Thus, weak biases on $\langle\omega\rangle_\Lambda$ can be greatly effective at directing the protocol sampling toward the optimum.

Gaussian fluctuations

We have computed $S(\omega)$ for the spin inversion process both with and without the simplifying assumption that the dissipation is Gaussian distributed. We find that the Gaussian approximation provides an estimate that is accurate within statistical error despite requiring a significantly reduced number of trajectories. To more explicitly demonstrate the validity of the approximation, we randomly selected three protocols from ensembles at different values of γ , which are shown in Fig. 3(a). For each protocol, we computed the dissipation distribution $P(\omega|\Lambda)$. Empirically, we find that dissipation distributions are strikingly Gaussian over a large range of ω that includes $\omega = 0$. At large positive values of dissipation, we observe “fat” exponential tails, consistent with the structure of generic current large deviation functions with time-independent drive [38, 39]. This fat tail, associated with clusters of spins that resist reorientation, does not degrade our use of the Gaussian dissipation assumption. The positive λ bias, useful to study low-dissipation behavior, focuses the sampling towards the Gaussian region of the distribution, not the exponential tails where the statistical weight is negligible even for $\lambda = 0$.

DISCUSSION

Constructing protocol ensembles offers pragmatic advantages over determining strictly optimal driving procedures. In simple model systems that can be optimized exactly, minimum-dissipation protocols can involve features that are singular or may be impractical to implement [14]. In such cases, the collection of near-optimal protocols becomes a natural target for design. A survey of this low-dissipation ensemble can additionally reveal which protocol parameters require the most precise tuning. Heuristically, it is less crucial to control those parameters with large fluctuations. Studying this ensemble also offers conceptual advantages. Efficient but sub-optimal nonequilibrium transformations are almost certainly the norm in biology at many scales. Indeed, the evolutionary dynamics of biological adaptation might be viewed

as an importance sampling on the space of protocols, roughly akin to the sampling methods developed in this paper. The surprising, often eccentric strategies used to perform simple tasks in biology are, perhaps, indicative of the myriad options provided by an ensemble of protocols evolving under a complex set of constraints.

MATERIALS AND METHODS

We sample the joint space of trajectories and protocols using Markov Chain Monte Carlo. Each point in this space consists of a protocol and N independent trajectories subject to that protocol. With tunable bias λ , the Markov chain samples the distribution, (5). For the 2D Ising example, protocols are parametrized by the values of the temperature and external field at 11 evenly spaced times. We call the values at these special times the control points. Between any two neighboring control points the temperature and field strength are linearly interpolated. Each Monte Carlo move first attempts to adjust the protocol by moving a single control point by a random displacement in the temperature-field plane. The move is constructed to be symmetric, meaning the probability of selecting any displacement vector equals the probability of a displacement of the opposite sign. Using this trial protocol, N new trajectories are simulated using a sequence of Glauber single-spin flips. Conventionally, each step of the Monte Carlo dynamics chooses a random spin and that spin is flipped to generate a trial configuration. To enable more efficient noise-guided trajectory sampling, we use a modified Ising dynamics: the trial configuration is given by setting the randomly selected spin to either the up or the down state without reference to its prior state [31]. The move is futile when the selected spin is already in the trial configuration. Since half of the moves are futile on average, the Monte Carlo time is rescaled by a factor of two as compared to ordinary single-spin-flip Glauber dynamics. Following each move, the probability of running that step backwards is computed, enabling an explicit calculation of the dissipation of each trajectory. The new protocol and trajectories are conditionally accepted with probability $\min[1, \exp(-\lambda\Delta\bar{\omega})]$, where $\Delta\bar{\omega}$ is the difference between the sample means under the original and trial protocols.

The protocol entropy is calculated, up to a constant offset $\ln\Omega_0$, using a weighted average over the protocols collected by the Monte Carlo procedure,

$$S(\omega) = \ln \left[\Omega_0 \int d\Lambda(t) \frac{P_{\text{sampled}}[\Lambda(t)]}{\langle e^{-\lambda\omega/N} \rangle_\Lambda^N} \delta(\omega - \langle\omega\rangle_\Lambda) \right]. \quad (11)$$

From a set of M sampled protocols,

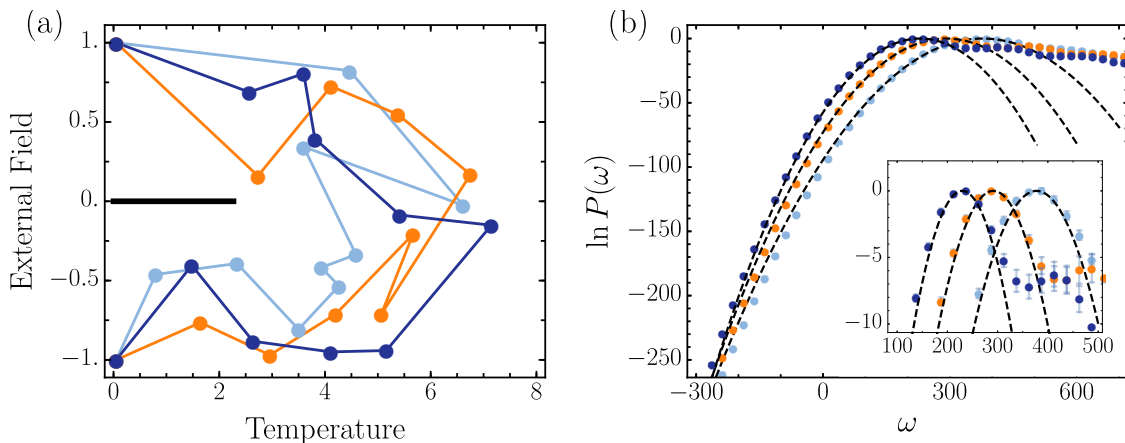


FIG. 3. *Dissipation distributions for representative protocols.* (a) Three randomly selected protocols from the ensemble (5) are plotted on the temperature, external field plane as in Fig. 1. (b) The distribution of dissipation values $P(\omega|\Lambda)$ for the three protocols, displayed with corresponding colors. Dashed black lines show Gaussian distributions with the same means $\langle\omega\rangle_\Lambda$ as the sampled distributions and with variances $2\langle\omega\rangle_\Lambda$. Inset: The neighborhood around the average dissipation values is shown in greater detail.

$\{\Lambda_1, \Lambda_2, \dots, \Lambda_\alpha, \dots, \Lambda_M\}$, we therefore estimate

$$S(\omega) = \ln \left[\frac{\Omega_0}{M} \sum_{\alpha=1}^M \frac{\delta(\omega - \langle\omega\rangle_{\Lambda_\alpha})}{\langle e^{-\lambda\omega/N} \rangle_{\Lambda_\alpha}^N} \right]. \quad (12)$$

Operationally, this amounts to collecting a histogram of values of $\langle\omega\rangle_\Lambda$ with each entry weighted by the corresponding value of $\langle e^{-\lambda\omega/N} \rangle_{\Lambda_\alpha}^N$. To generate Fig. 2, each of these weights is computed by estimating the exponential average from 1000 independent trajectories. In practice, $S(\omega)$ is constructed using the MBAR method to combining samples collected with $N = 20$ and with several different values of the bias ranging from $\lambda = 0$ to $\lambda = 1$. The offset $\ln \Omega_0$ is chosen such that $S(\omega)$ is zero at its maximum.

The protocol entropy can be computed much more efficiently when the Gaussian approximation may be used to evaluate the exponential average. To evaluate the validity of this approximation for the Ising dynamics, we compute the actual dissipation distributions by sampling trajectories with a fixed protocol. These trajectories are umbrella sampled using harmonic biases, which restrain the dissipation to fluctuate around a specified value. By choosing several different harmonic biases, trajectories were biased into both tails of the dissipation distribution, which was reconstructing using the MBAR method [37].

When the Gaussian approximation is appropriate, it is also wasteful to use a large value of N . Low-dissipation protocols may be sampled with an effective biasing strength $\gamma = \lambda(1 - \lambda/N)$ using various combinations of N and λ , and a small N reduces the computational expense. However, when N is too small or λ too large, the Monte Carlo acceptance probability drops precipitously, a fact elaborated upon in the SI. Sampling efficiency is

poor under these conditions because the Markov chain favors a collection of rare trajectories with dissipation below the mean (and often below zero). This issue can be partially alleviated by introducing replica exchange moves—random swaps exchanging replicas with different biasing strengths λ . The implementation of this procedure naturally mirrors the use of replica exchange to surmount kinetic traps when sampling low-temperature molecular configurations. Further performance enhancements are obtained when trial trajectories are generated with random numbers (noises) which correlate with the noises of the previous collection of trajectories. An implementation of this noise-guided sampling is described in detail elsewhere [31, 40]. The noise guidance technique is not strictly required to perform the protocol sampling, but in the SI we show that it can provide significant practical benefits.

ACKNOWLEDGMENTS

TRG acknowledges support from the NSF Graduate Research Fellowship, the Fannie and John Hertz Foundation, and the Gordon and Betty Moore Foundation as an MIT Physics of Living Systems Fellow. GMR would like to acknowledge support from the NSF Graduate Research Fellowship. PLG was supported by the U.S. Department of Energy, Office of Basic Energy Sciences, through the Chemical Sciences Division (CSD) of the Lawrence Berkeley National Laboratory (LBNL), under Contract DE-AC02-05CH11231. GEC acknowledges support from the U.S. Army Research Laboratory and the U.S. Army Research Office under Contract No. W911NF-13-1-0390.

* toddging@mit.edu
† rotskoff@berkeley.edu
‡ GECrooks@lbl.gov
§ geissler@berkeley.edu

[1] S. B. Smith, L. Finzi, and C. Bustamante, *Science* **258**, 1122 (1992).
[2] J. Liphardt, S. Dumont, S. B. Smith, I. Tinoco Jr., and C. Bustamante, *Science* **296**, 1832 (2002).
[3] D. Collin, F. Ritort, C. Jarzynski, S. B. Smith, I. Tinoco, and C. Bustamante, *Nature* **437**, 231 (2005).
[4] I. A. Martínez, E. Roldán, L. Dinis, D. Petrov, J. M. R. Parrondo, and R. A. Rica, *Nat. Phys.* **12**, 67 (2016).
[5] V. Blickle and C. Bechinger, *Nat. Phys.* **8**, 143 (2012).
[6] S. Toyabe, T. Sagawa, M. Ueda, E. Muneyuki, and M. Sano, *Nat. Phys.* **6**, 988 (2010).
[7] Y. Jun, M. Gavrilov, and J. Bechhoefer, *Phys. Rev. Lett.* **113**, 190601 (2014).
[8] C. Jarzynski, *Phys. Rev. Lett.* **78**, 2690 (1997).
[9] G. E. Crooks, *Excursions in statistical dynamics*, Ph.D. thesis, University of California at Berkeley (1999).
[10] R. Spinney and I. Ford, “Fluctuation relations: A pedagogical overview,” in *Nonequilibrium Statistical Physics of Small Systems* (Wiley-VCH Verlag GmbH & Co. KGaA, 2013) pp. 3–56.
[11] F. Weinhold, *J. Chem. Phys.* **63**, 2479 (1975).
[12] G. Ruppeiner, *Phys. Rev. A* **20**, 1608 (1979).
[13] P. Salamon, A. Nitzan, B. Andresen, and R. S. Berry, *Phys. Rev. A* **21**, 2115 (1980).
[14] T. Schmiedl and U. Seifert, *Phys. Rev. Lett.* **98**, 108301 (2007).
[15] A. Gomez-Marin, T. Schmiedl, and U. Seifert, *J. Chem. Phys.* **129**, 024114 (2008).
[16] H. Then and A. Engel, *Phys. Rev. E* **77**, 041105 (2008).
[17] P. R. Zulkowski, D. A. Sivak, G. E. Crooks, and M. R. DeWeese, *Phys. Rev. E* **86**, 041148 (2012).
[18] P. R. Zulkowski and M. R. DeWeese, *Phys. Rev. E* **92**, 032117 (2015).
[19] P. Maragakis, F. Ritort, C. Bustamante, M. Karplus, and G. E. Crooks, *J. Chem. Phys.* **129**, 024102 (2008).
[20] C. Dellago and G. Hummer, *Entropy* **16**, 41 (2013).
[21] G. Oster and H. Wang, *J. Bioenerg. Biomembr.* **32**, 459 (2000).
[22] B. Lambson, D. Carlton, and J. Bokor, *Phys. Rev. Lett.* **107**, 010604 (2011).
[23] J. Hong, B. Lambson, S. Dhuey, and J. Bokor, *Sci. Adv.* **2**, e1501492 (2016).
[24] C. Andrieu and G. O. Roberts, *Ann. Stat.* , 697 (2009).
[25] R. C. Ball, T. M. A. Fink, and N. E. Bowler, *Phys. Rev. Lett.* **91**, 030201 (2003).
[26] M. A. Beaumont, *Genetics* **164**, 1139 (2003).
[27] D. M. Ceperley and M. Dewing, *J. Chem. Phys.* **110**, 9812 (1999).
[28] L. Lin, K. F. Liu, and J. Sloan, *Phys. Rev. D* **61**, 074505 (2000).
[29] C. Dellago, P. G. Bolhuis, and D. Chandler, *J. Chem. Phys.* **108**, 9236 (1998).
[30] G. E. Crooks and D. Chandler, *Phys. Rev. E* **64**, 026109 (2001).
[31] T. R. Gingrich and P. L. Geissler, *J. Chem. Phys.* **142**, 234104 (2015).
[32] T. Speck and U. Seifert, *Phys. Rev. E* **70**, 066112 (2004).

[33] O. Mazonka and C. Jarzynski, arXiv preprint cond-mat/9912121 (1999).
[34] J. L. Lebowitz and H. Spohn, *J. Stat. Phys.* **95**, 333 (1999).
[35] M. Venturoli, E. Vanden-Eijnden, and G. Ciccotti, *J. Math. Chem.* **45**, 188 (2009).
[36] G. M. Rotskoff and G. E. Crooks, *Phys. Rev. E* **92**, 060102 (2015).
[37] M. R. Shirts and J. D. Chodera, *J. Chem. Phys.* **129**, 124105 (2008).
[38] T. R. Gingrich, J. M. Horowitz, N. Perunov, and J. L. England, *Phys. Rev. Lett.* **116**, 120601 (2016).
[39] P. Pietzonka, A. C. Barato, and U. Seifert, arXiv preprint arXiv:1512.01221 (2015).
[40] T. R. Gingrich, *Two Paths Diverged: Exploring Trajectories, Protocols, and Dynamic Phases*, Ph.D. thesis, University of California at Berkeley (2015).

SUPPORTING INFORMATION (SI)

Sampling efficiency

Ergodic sampling of $P_{\text{canon}}[\Lambda(t)]$ requires that decorrelated protocols be generated, and the efficiency of the sampling depends on how many Monte Carlo moves are required to produce each decorrelated sample. As discussed in the main text, the canonical distribution with bias γ may be accessed with various choices of N and λ , yet the sampling efficiency depends on these choices. A large value of N bears a clear computational cost since N new trajectories must be simulated for each trial protocol. It is not, however, always optimal to choose the minimal N capable of generating bias γ , $N^* = \text{Ceil}(4\gamma)$. The problem with using a small value of N is that rare low-dissipation trajectories (including those with negative dissipation) can depress the probability of accepting a protocol move, even when the trial protocol has a lower *average* dissipation. The smaller the choice of N , the more rare trajectories influence the acceptance of protocol moves. Consequently, the optimal choice of N often exceeds N^* .

In practice, the best choice of N depends on the Monte Carlo moves used to update trajectories and protocols. For example, there is a trade-off in choosing the best protocol space moves. Large changes to the protocol have a low acceptance probability, but small steps require many moves before sampling a protocol with a decorrelated value of mean dissipation. To quantify the trade-offs between possible choices of N and of Monte Carlo moves, we construct a correlation function:

$$C_{\omega}(j) = \left\langle \delta \langle \omega \rangle_{\Lambda_i} \delta \langle \omega \rangle_{\Lambda_{i+j}} \right\rangle, \quad (\text{S1})$$

where $\delta \langle \omega \rangle_{\Lambda(i)}$ is the difference between the i^{th} sampled protocol’s average dissipation and the mean dissipation, found by averaging over all protocols in the ensemble. Assuming exponentially decaying correlations

($C_\omega(j)/C_\omega(0) = e^{-j/\tau_\omega}$), we set the correlation time to the decay constant τ_ω . This decorrelation time is the typical number of protocols which must be sampled before generating a protocol with a decorrelated value of the mean dissipation. Since each new protocol must be accompanied by the simulation of N new trajectories, the computational cost for obtaining each decorrelated sample is given by $N\tau_\omega$.

The decorrelation time τ_ω implicitly depends on N as well as on the details of the sampling moves. To gain intuition about the most computationally-efficient choice of N , we first consider a simplified Gaussian model. For this model, the optimal N slightly exceeds N^* . The Ising dynamics is more complicated, requiring τ_ω to be computed from simulations. We show that the computational expense depends on N in a similar manner as in the Gaussian model, though the computational expense may be reduced by employing noise-guided path sampling.

Gaussian model

We sample a scalar protocol Λ in the vicinity of the minimum dissipation protocol Λ^* . The advantage of sampling near Λ^* is that we can Taylor expand to arrive at an expression for the average dissipation associated with a perturbation $\delta\Lambda = \Lambda - \Lambda^*$,

$$\langle\omega\rangle_\Lambda = \langle\omega\rangle_{\Lambda^*} + \frac{1}{2} \delta\Lambda \left. \frac{d^2 \langle\omega\rangle_\Lambda}{d\Lambda^2} \right|_{\Lambda^*} \delta\Lambda. \quad (\text{S2})$$

We assume that the dissipation distribution associated with a protocol Λ is Gaussian,

$$p(\omega|\Lambda) \propto \exp\left(-\frac{(\omega - \langle\omega\rangle_\Lambda)^2}{4\langle\omega\rangle_\Lambda}\right). \quad (\text{S3})$$

We furthermore use a Gaussian distribution to propose a trial protocol,

$$P(\Lambda_i \rightarrow \Lambda_{i+1}) \propto \exp\left(-\frac{(\Lambda_i - \Lambda_{i+1})^2}{2D^2}\right). \quad (\text{S4})$$

Using the new trial protocol, the dissipation for N independent trajectories is drawn from (S3) to compute the sample mean dissipation for the new protocol $\bar{\omega}$. For a choice of bias γ , we choose λ and N such that $\gamma = \lambda(1 - \lambda/N)$ and accept the new protocol and trajectories with probability

$$P_{\text{accept}}^{\Lambda \rightarrow \Lambda'} = \min[1, e^{-\lambda\Delta\bar{\omega}}], \quad (\text{S5})$$

where $\Delta\bar{\omega}$ is the difference between the new protocol's sample mean dissipation and that of the old protocol and trajectories.

The correlation between subsequent samples is given by

$$C_\omega(1) = \int d\Lambda_i \int d\Lambda_{i+1} P(\Lambda_i) P(\Lambda_i \rightarrow \Lambda_{i+1}) \delta\langle\omega\rangle_{\Lambda_i} \\ \times \left(P_{\text{accept}}^{\Lambda_i \rightarrow \Lambda_{i+1}} \delta\langle\omega\rangle_{\Lambda_{i+1}} + \left(1 - P_{\text{accept}}^{\Lambda_i \rightarrow \Lambda_{i+1}}\right) \delta\langle\omega\rangle_{\Lambda_i} \right). \quad (\text{S6})$$

with

$$P_{\text{accept}}^{\Lambda_i \rightarrow \Lambda_{i+1}} = \int_{-\infty}^0 d\Delta\bar{\omega} P(\Delta\bar{\omega}|\Lambda_i, \Lambda_{i+1}) \\ + \int_0^\infty d\Delta\bar{\omega} P(\Delta\bar{\omega}|\Lambda_i, \Lambda_{i+1}) e^{-\lambda\Delta\bar{\omega}} \quad (\text{S7})$$

giving the acceptance probability for the Monte Carlo protocol move. Since the sample mean dissipations (for both the old and trial protocol) are Gaussian distributed, $P(\Delta\bar{\omega}|\Lambda_i, \Lambda_{i+1})$ is also a Gaussian,

$$P(\Delta\bar{\omega}|\Lambda_i, \Lambda_{i+1}) \propto \\ \exp\left(-\frac{N\left(\Delta\bar{\omega} - \left(\langle\omega\rangle_{\Lambda_{i+1}} - \left(1 - \frac{2\lambda}{N}\right)\langle\omega\rangle_{\Lambda_i}\right)\right)^2}{4\left(\langle\omega\rangle_{\Lambda_i} + \langle\omega\rangle_{\Lambda_{i+1}}\right)}\right). \quad (\text{S8})$$

The acceptance rate may therefore be expressed in terms of error functions. The number of attempted protocol moves required to sample protocols with decorrelated mean dissipations is given by $\tau_\omega = -1/\ln(C_\omega(1)/C_\omega(0))$. A complicated integral expression for τ_ω in terms of $\langle\omega\rangle_{\Lambda^*}$, D , γ , and N may be derived in terms of error functions. Numerically evaluating the integral expression yields the N -dependence of the computational cost, $N\tau_\omega$, for generating protocols with decorrelated average dissipation. Analogously, we may compute the time to find decorrelated values of the scalar protocol τ_Λ as the decay constant for the correlation function

$$C_\Lambda(j) = \langle\delta\Lambda_i \delta\Lambda_{i+j}\rangle. \quad (\text{S9})$$

Both τ_ω and τ_Λ yield the same heuristic: the computational expense is minimal when N slightly exceeds N^* , as plotted in Fig. S1.

Ising dynamics

Using various choices of λ and N , the canonical protocol ensemble is sampled by a sequence of protocol moves which alter the control point at a single time. Either the control point's magnetic field strength is increased by a random uniform number between -0.5 and 0.5 or the temperature is increased by a random uniform number between -2.5 and 2.5 . The protocol move is resampled if the magnitude of the magnetic field strength at any

time exceeds 1 or if the dimensionless temperature exits the range $[0, 8]$. N trajectories are generated by repropagating forward dynamics from the initial time or by running time-reversed dynamics from the final time slice and reweighting the trajectories into the forward-trajectory ensemble. When noise guidance path sampling is not being used, each trial trajectory is generated by drawing new random noises to carry out the steps of the spin-flip dynamics. The noise guidance path sampling scheme recycles, with probability $1 - \epsilon$, each random number from the previous trajectory. Over time, each random number gets resampled uniformly, but the correlations between an old trajectory and a new trajectory are enhanced [31, 40].

To assess how rapidly the protocol space is sampled, protocols were stored and an accurate estimate of $\langle \omega \rangle_\Lambda$ was found by averaging over 1000 trajectories with the fixed protocol. Fig. S2(a) shows the (Monte Carlo) time series of this average dissipation. Using this time series, the correlation function $C(j)$ is computed for each choice

of N and λ . The correlation functions are fit to exponential decays, and the decay constant τ is extracted to yield the computational cost ($N\tau$) as a function of N . Fig. S3 illustrates that the optimal choice of N exceeds N^* , as in the Gaussian model. The noise guidance strategy aids small- N sampling, thereby lowering the optimal N . For these small choices of N , the noise guidance scheme offers a roughly order of magnitude speed up.

Sample mean fluctuations

The biasing strength γ necessary to sample protocols with dissipation $\langle \omega \rangle$ is given by the slope of $S(\omega)$ at $\omega = \langle \omega \rangle$. When $S(\omega)$ is especially steep, it therefore requires a very strong bias to access the low-dissipation entropy. Sampling efficiency worsens for large γ , so we note an alternative method for computing $S(\omega)$ that makes use of the fluctuations in the sample mean of N trajectories.

We define the entropy $\bar{S}(\omega)$ to give the density of protocols and trajectories which have a sample mean dissipation within an infinitesimal window of ω :

$$\bar{S}(\omega) = \ln \left[\bar{\Omega}_0 \int d\Lambda(t) dx_1(t) \dots dx_N(t) \delta \left(\sum_i \frac{\omega[x_i(t), \Lambda]}{N} - \bar{\omega}_\Lambda \right) \right]. \quad (\text{S10})$$

In the limit $N \rightarrow \infty$ this entropy must converge to the protocol entropy, $S(\omega)$, but $\bar{S}(\omega)$ falls off less rapidly around the minimal average dissipation. The tails of $\bar{S}(\omega)$ with low sample mean may therefore be umbrella sampled bias λ more modest than the bias γ which would be necessary to sample $S(\omega)$ directly. By making the

Gaussian approximation, we can reconstruct $S(\omega)$ from N -dependence of $\bar{S}(\omega)$ using

$$\bar{S}(\omega) = \ln \left[\bar{\Omega}_0 \int d\omega \exp \left(-\frac{N(\bar{\omega} - \omega)^2}{4\omega} + S(\omega) \right) \right], \quad (\text{S11})$$

a technique illustrated in Fig. S4.

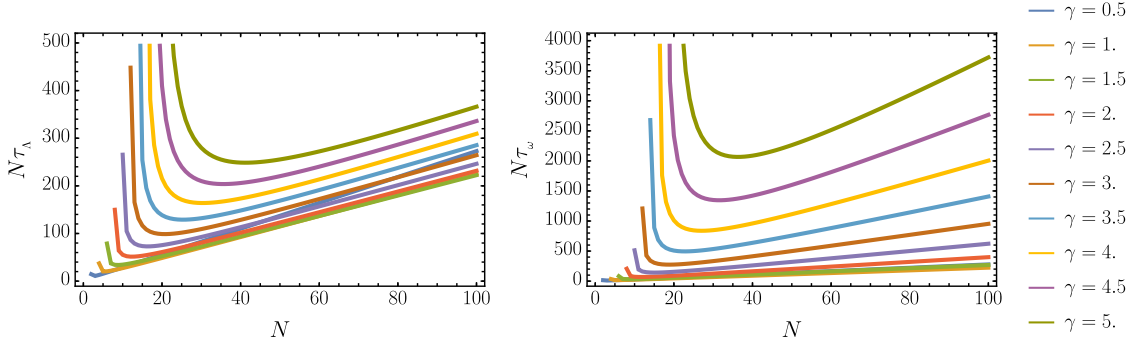


FIG. S1. *Computational expense of sampling varies non-monotonically with N .* (Left) Computational cost, in number of trajectories needed to generate a decorrelated protocol, for the Gaussian model with various values of the bias γ . (Right) Cost to generate protocols with a decorrelated value of the mean dissipation.

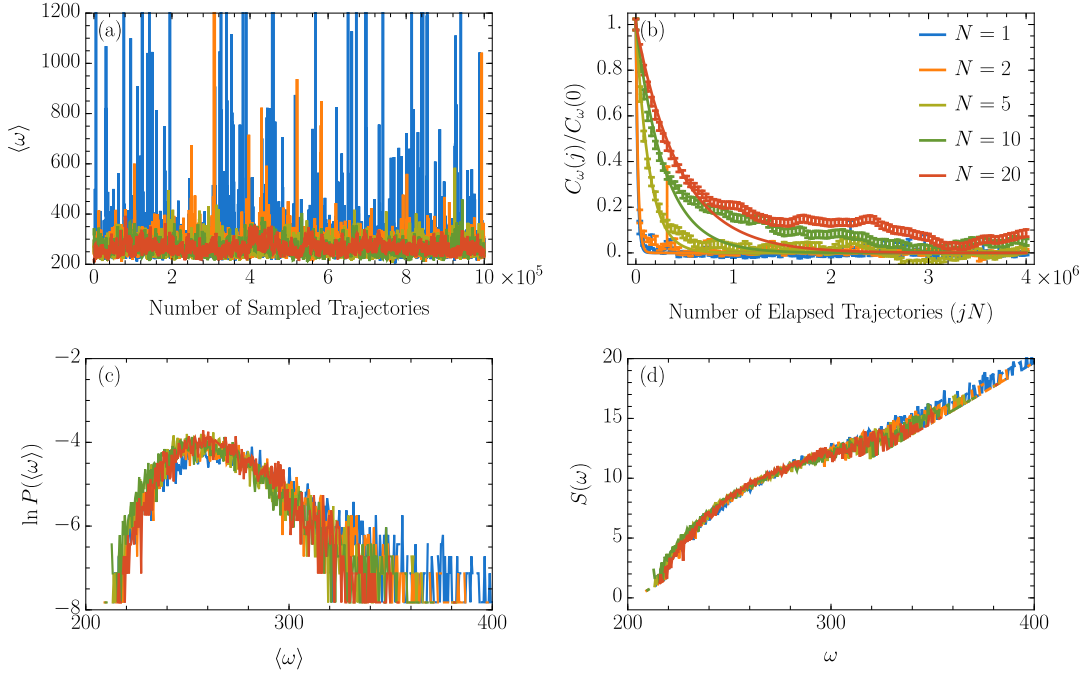


FIG. S2. *Sampling $e^{-\gamma\langle\omega\rangle\Lambda}$ with $\gamma = 0.1$ and various choices of N .* To analyze the marginal protocol distributions generated from different choices of N (these marginal distributions agree with each other in the Gaussian dissipation distribution limit), we report on the statistics of $\langle\omega\rangle_\Lambda$, estimated as a sample mean of 1000 independent trajectories. (a) Fluctuations in this mean dissipation for different sampled protocols. The x -axis measures “time” for the protocol sampling MC procedure by counting the total number of simulated spin-flip trajectories (which differs from the total number of sampled protocols by a factor of N). Counting the number of trajectories roughly reflects the computational expense. (b) Correlation functions showing how many trajectories must be simulated before a new protocol is produced with a statistically uncorrelated value of the mean dissipation. Using large values of N can be unnecessarily wasteful because each protocol requires sampling N more trajectories. (c) Histogram of the sampled average dissipation values. Note that the different choices of N produce the same distributions except that extreme events can be over-represented by small- N sampling. (d) The histogram of (c) is reweighted to yield the protocol entropy. In the neighborhood of the histogram’s peak the protocol entropy calculation is robust to errors from small- N sampling. By choosing various biasing strengths γ , we highlight different ranges of $\langle\omega\rangle$ and stitch them together to compute the protocol entropy curve reported in the main text.

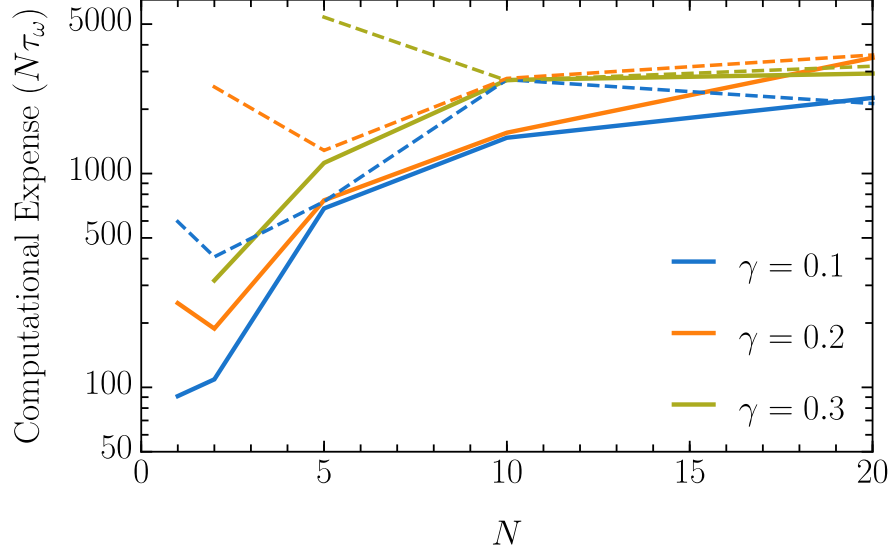


FIG. S3. *Computational expense of generating decorrelated protocols.* For various N and γ , an exponential time constant τ was extracted from the correlation functions plotted in Fig. S2(b) to obtain the number of trajectories which must be simulated to obtain a decorrelated protocol. This computational expense depends not only on N and γ but also on the manner in which new trajectories are generated. The dashed lines show the expense when each trajectory is drawn at random. Solid lines show the improvement that can be achieved by using noise guidance. When generating a new Ising trajectory, the noise guidance scheme re-used each of the previous trajectory's random numbers with probability 0.999 ($\epsilon = 10^{-3}$).

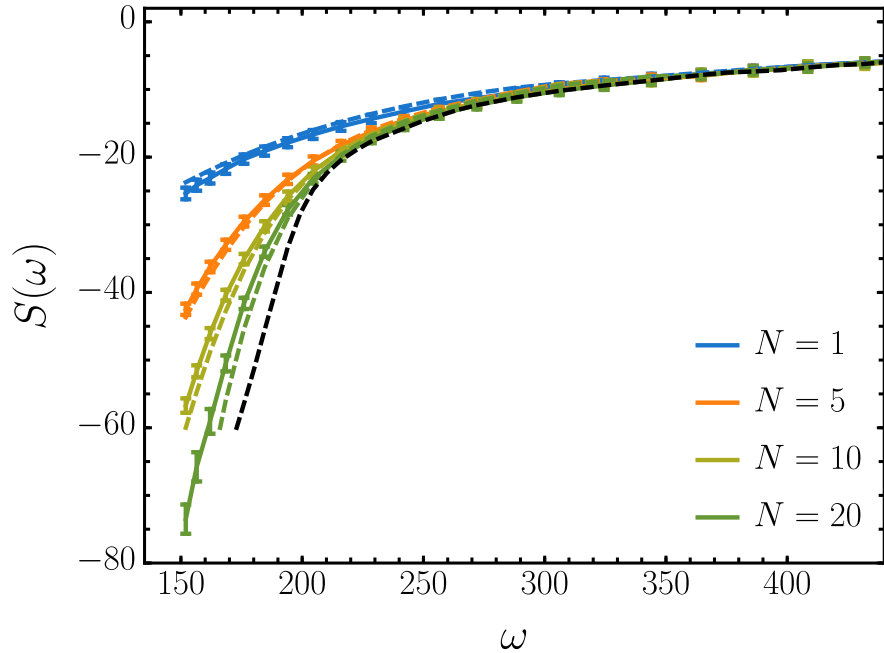


FIG. S4. *Inferring protocol entropy from finite N sampling.* The colored lines with error bars show $\bar{S}(\omega)$ for four choices of N , computed using MBAR to combine sampling with various choices of γ . The form of $S(\omega)$ is inferred (black dashed line) by fitting to (S11) for $N = 1, 5, 10, 20$. The dashed colored lines show the expected $\bar{S}(\omega)$ given the inferred protocol entropy. It is typically harder to sample in regions where $\bar{S}(\omega)$ is steep. Since the entropy is less steep for small N , it can be productive to compute $\bar{S}(\omega)$ with modest N then infer the $N \rightarrow \infty$ limit $S(\omega)$.